Finite-Time Fault-Tolerant Formation Control for Distributed Multi-Vehicle Networks with Bearing Measurements

Kefan Wu, *Student Member, IEEE*, Junyan Hu, *Member, IEEE*, Zhengtao Ding, *Senior Member, IEEE*, and Farshad Arvin, *Senior Member, IEEE*

***Abstract*—This paper addresses a bearing-only formation tracking problem in robotic networks by considering exogenous disturbances and actuator faults. In contrast to traditional position-based coordination strategies, the bearing-only coordinated movements of the unmanned vehicles only rely on the neighboring bearing information. This feature can be utilized to reduce the sensing requirements in the hardware implementation. A gradient-descent protocol is first developed to achieve the desired coordination within a prespecified settling time, where the unknown disturbances are considered in the vehicle dynamics, then the bound of formation tracking error is guaranteed by the Lyapunov approach. In case of damage to the actuators (e.g., motors) in some of the vehicles during the task, fault-tolerant analysis of the proposed controller is provided to ensure the success of the task in extreme environments. Furthermore, the proposed bearing-based method is extended to deal with general linear systems, which can be applied to a wider range of robotic platforms. Finally, numerical simulations and lab-based experiments using unmanned ground vehicles are conducted to validate the effectiveness of the proposed strategy.**

***Note to Practitioners*—The aim of this paper is to develop and design a practical bearing-only formation control approach for multi-vehicle systems. Many real-world complex tasks can be solved by multiple unmanned aerial and ground vehicles being connected by a communication network. This paper has proposed a formation tracking scheme for networked multi-vehicle systems that only relies on the relative bearing information of the neighboring vehicles. Closed-loop stability of the scheme and finite-time convergence of the tracking error have been established using the Lyapunov stability approach. The proposed method ensures the robustness and fault-tolerance of the multi-vehicle system against hardware faults or exogenous disturbances. A systematic set of guidelines on how to apply the proposed strategy in practice is also provided for the control practitioners in the form of an algorithm. In order to demonstrate the feasibility and usefulness of the proposed coordination scheme, numerical simulations and lab-based hardware experiments were conducted. Potential applications of the proposed scheme include search and rescue, security surveillance and cooperative exploration.**

***Index Terms*—Distributed control, multi-vehicle systems, finite-time consensus, swarm robotics, bearing-based formation.**

This work was partially supported by the EU H2020-FET RoboRoyale (964492).

K. Wu and Z. Ding are with the Department of Electrical and Electronic Engineering, The University of Manchester, Manchester, M13 9PL, U.K. (e-mail: {kefan.wu; zhengtao.ding}@manchester.ac.uk)

J. Hu is with the Department of Computer Science, University College London, London, WC1E 6BT, U.K. (e-mail: junyan.hu@ucl.ac.uk)

F. Arvin is with the Department of Computer Science, Durham University, Durham, DH1 3LE, U.K. (e-mail: farshad.arvin@durham.ac.uk)

I. Introduction

Formation in robotic networks has received great attention from robotics and automation communities. Motivated by commonly observed collective behaviors of animals, distributed control on formation tasks aims to coordinate a team of unmanned vehicles to form a desired geometric pattern through local information. Cooperative control methods have been widely used in practical robotic applications, such as collaborative manipulators [1], object transportation [2], search and rescue [3]–[5], ecosystem hacking using micro-robot swarms [6], exploration in unknown environments [7], autonomous vehicle platooning [8]–[10], etc. This motivates researchers to develop advanced coordination strategies for multi-vehicle systems.

Among all the distributed formation control methods proposed in the last decade, one of the major approaches to deal with multi-vehicle formation tracking problems is position measurement [11]. As an example, distance-based multi-robot formation control was explored in [12] by utilizing the goal assignment. A distributed estimation and formation control problem was addressed in [13] with guaranteed performance. The article [14] has laid a major contribution in the area of fault-tolerant formation control design, where an event-triggered control scheme was developed for autonomous surface vehicles under malicious attacks. In another study, Hu et al. [15] proposed a robust formation control protocol for multiple mobile robots based on negative imaginary dynamics. Bio-inspired formation control for unmanned aerial vehicle (UAV) swarms was analyzed in [16], where multiple leaders and switching topology were considered in the control system design. A fault-tolerant formation protocol was proposed for wheeled mobile robots in [17]. The authors in [18] employed the radial basis function neural networks and sliding-mode PID controller to deal with the fault-tolerant issue for heterogeneous vehicular platoons. However, in the aforementioned studies, the proposed coordinated controllers depend on the assumption that the relative distances or positions among the neighbors are detectable, which requires high quality sensory outputs that may not be easily fulfilled in extreme environments.

To overcome these limitations, bearing-only control techniques have been explored by researchers in recent years. Only the neighboring bearings of vehicles are required to realize the desired goal by implementing bearing-only protocols. Some

preliminary results on bearing-based formation control have been developed in [19]–[23]. During the hardware implementation, the bearing information can be detected by wireless vision-based sensors [24]. Therefore, the design of bearing-only control shows the promising capacity to achieve multi-vehicle formation tasks by using on-board sensors. There are two main methods in bearing-only cooperative control, the first is controlling the bearing angles. In this regard, triangular formations were first discussed in [25]. The authors in [26] studied cyclic formations. However, they were constrained in 2-D space. The second strategy is coordinating the bearing vectors. The bearing rigidity theory was proposed in [20], which is a strong method to study the properties of the target formation. The gradient-descent (GD) bearing-only protocol was proposed in [27] for stability analysis. Furthermore, Zhao et al. [22] proposed bearing-only control law by GD method to handle double-integrator and unicycles systems. Since exogenous disturbances may appear in the dynamics of the vehicles, the coordination problems become more challenging. In [22], an integral term was introduced in the control protocol to handle the exogenous disturbance. The authors in [28] verified that the formation error could exponentially converge to a bounded set with bounded exogenous disturbance. In the follow up study [29], the upper-bound of the tracking error was computed and then the correlation between system factors were discussed. However, in the aforementioned works, only global asymptotic stability can be ensured, which means that the target geometric pattern cannot be formed within a finite time period.

Another important indicator of performance is the settling time of the cooperation task. As a result, the finite-time control techniques have been extensively explored in multi-agent systems (see [30]–[32]). In [30], the fixed-time formation tracking for networked agents with uncertain dynamics was addressed. In another study [33], the authors proposed a fixed-time protocol based on output feedback. Finite-time convergence analysis is nontrivial for bearing-only control. The authors in [26], [34], [35] proposed several finite-time bearing-only (FTBO) coordination protocols. However, the convergence time is affected by the initial states. The designed control inputs are not smooth as they contain signum functions and fractional power feedback. Besides, unknown and actuator faults were not considered in the vehicles' dynamics, which may not provide reliable performance in real-world applications. In other words, how to design FTBO formation control with smooth control inputs, exogenous disturbances, and actuator faults remains an open problem.

Motivated by the advancements and challenges in bearing-only formation tracking problems, in this paper, a novel fault-tolerant FTBO protocol is proposed for multi-vehicle networks with exogenous disturbances and actuator faults. This bearing-based controller can minimize the sensing requirements of each vehicle compared with traditional position-based method (see [3], [11], [13], [36]). Different from most works related to finite-time control strategies (see [30], [32]), the multi-vehicle formation can be accomplished within a given finite time that can be predefined by users by implementing the designed algorithm. Then, in comparison with [31], the exogenous disturbance and the actuator failures are considered in the multi-vehicle system. Via Lyapunov stability analysis, a sufficient condition is presented to show that the formation error will converge to a bounded set if a bounded exogenous disturbance appears in the vehicle dynamics. Besides, we also extend the proposed results to deal with linear time-invariant (LTI) dynamics, which is more practical compared to first-order and second-order systems that are often considered in the bearing-only coordination problems. To the best of authors' observation, such a novel protocol design has not been reported by researchers in the literature. The contribution of this paper can be summarized as:

- A bearing-only formation coordination protocol is proposed for multi-vehicle networks. In contrast to traditional position-based coordination strategies, the coordinated movement of each vehicle only requires the neighboring bearings, which significantly reduces the sensing requirements.
- A novel GD coordination law is proposed to realize the desired geometric pattern within a prespecified converge time that can be selected by users. Different from most studies in the area of bearing-only control, the proposed method can also be used to deal with LTI dynamics.
- Exogenous disturbances and actuator faults are considered in the protocol design. It has been proved that the formation tracking error will converge to a bounded set for unknown exogenous disturbances and actuator faults.

II. Problem Formulation

A. Notations and Preliminaries

Consider n networked mobile vehicles (which include n_l leaders and n_f followers) in $\mathbb{R}^d$ ($n \geq 2$, $d \geq 2$ and $n_l + n_f = n$). The *configuration* of the vehicles can be denoted as $p = \mathrm{col}(p_1, \cdots, p_n)$. Let the undirected graph $\mathcal{G} = (\mathcal{V}, \mathcal{E})$ denote the communication among the vehicles. $\mathcal{V}_l = \{v_1, \ldots, v_{n_l}\}$ denoted leaders' set, and $\mathcal{V}_f = \{v_{n_l+1}, \ldots, v_n\}$ denotes followers' set, respectively, and $\mathcal{V} = \mathcal{V}_l \cup \mathcal{V}_f$. The edge set is denoted by $\mathcal{E} \subseteq \mathcal{V} \times \mathcal{V}$. The edge $(i, j) \in \mathcal{E}$ indicates that vehicle i can obtain the relative bearing from vehicle j, such that vehicle j is a neighbor of i. Let $\mathcal{N}_i = \{j \in \mathcal{V} : (i, j) \in \mathcal{E}\}$ be the neighbor set of vehicle i. Since the graph is undirected, we have $(i, j) \in \mathcal{E} \Leftrightarrow (j, i) \in \mathcal{E}$ [37].

Let $H_{ki} \in \mathbb{R}^{m \times n}$ (m is the number of the undirected edges) be the incidence matrix of the oriented graph (undirected graph $\mathcal{G}$ with orientation), where

$$[H]_{ki} = \begin{cases} 1, & i \text{ is the head of } k, \\ -1, & i \text{ is the tail of } k \\ 0, & \text{otherwise.} \end{cases}$$

The relative *edge vector* and *bearing vector* of p_j with respect to p_i can be defined as

$$e_{ij} := p_j - p_i, \quad g_{ij} := \frac{e_{ij}}{\|e_{ij}\|},$$

where $\|\cdot\|$ denotes the Euclidean norm of a vector or the spectral norm of a matrix. Define

$$P_{g_{ij}} := I_d - g_{ij}g_{ij}^{\mathrm{T}} \in \mathbb{R}^{d\times d},$$

where $I_d \in \mathbb{R}^{d\times d}$ denotes the identity matrix. It is obvious that $P_{g_{ij}} \geq 0$, $P_{g_{ij}}^2 = P_{g_{ij}}$, and $\mathrm{Null}(P_{g_{ij}}) = \mathrm{span}\{g_{ij}\}$. Then, we can imply that $\forall x \in \mathbb{R}^d, x$ is parallel to g_{ij} if and only if $P_{g_{ij}}x = 0$. This property is significant to design the controller via bearing measurement [19], [20]. Then we have

$$\dot{g}_{ij} = \frac{P_{g_{ij}}}{\|e_{ij}\|}\dot{e}_{ij}.$$

It can be seen that $g_{ij}^\top \dot{g}_{ij} = e_{ij}^\top \dot{g}_{ij} = 0$ due to the fact that $P_{g_{ij}}g_{ij} = 0$.

Let the edge (i,j) correspond to the kth ($k \in \{1,2,\cdots,m\}$) directed edge in oriented graph. For kth directed edge, we can redefine the edge and bearing vector as

$$e_k := e_{ij} = p_j - p_i, \quad g_k := \frac{e_k}{\|e_k\|}.$$

Similarly, we have $g_k^\top \dot{g}_k = 0$ and $e_k^\top \dot{g}_k = 0$. Then, we can conclude that $e = \mathrm{col}(e_1,\cdots,e_m) = (H \bigotimes I_d)p = \bar{H}p$.

Define the scale of the formation in the system as

$$\mathbf{s}(t) = \sqrt{\frac{1}{n}\sum_{i=1}^{n}\|p_i - \bar{p}\|^2} = \frac{\|p - \mathbf{1}_n \bigotimes \bar{p}\|}{\sqrt{n}},$$

where $\bar{p} = \frac{1}{n}(\mathbf{1}_n \bigotimes I_d)^\top p$ denotes the centroid of the formation.

Let $p^* = \mathrm{col}(p_1^*,\cdots,p_n^*)$ and $g^* = \mathrm{col}(g_1^*,\cdots,g_m^*)$ denote configuration and bearing vector of the goal formation $(\mathcal{G}, p^*)$. The *bearing Laplacian matrix* $\mathcal{B} \in \mathbb{R}^{dn\times dn}$ is introduced to characterize the properties of a formation. The block of $\mathcal{B}$ can be written as [20]

$$[\mathcal{B}]_{ij} = \begin{cases} \mathbf{0_{d\times d}}, & i \neq j,\ (i,j) \notin \mathcal{E}, \\ -P_{g_{ij}^*}, & i \neq j,\ (i,j) \in \mathcal{E}, \\ \sum_{k\in\mathcal{N}_i} P_{g_{ik}^*}, & i = j,\ i \in \mathcal{V}. \end{cases}$$

It is easy to see that $\mathcal{B} \geq 0$, $\mathcal{B}\mathbf{1}_{dn} = \mathcal{B}p^* = 0$, and $\mathcal{B} = \bar{H}^\top \mathrm{diag}(P_{g_k^*})\bar{H}$. The partition of $\mathcal{B}$ by leaders and followers is shown as

$$\mathcal{B} = \begin{bmatrix} \mathcal{B}_{ll} & \mathcal{B}_{lf} \\ \mathcal{B}_{lf}^\top & \mathcal{B}_{ff} \end{bmatrix} \tag{1}$$

where $\mathcal{B}_{ff} \in \mathbb{R}^{dn_f\times dn_f}$ and $\mathcal{B}_{ll} \in \mathbb{R}^{dn_l\times dn_l}$. In this paper, it is necessary to ensure that the target formation is unique. Hence, we present the following result.

Lemma 1. *[20] The desired formation can be uniquely determined by the bearing vectors $\{g_{ij}^*\}_{(i,j)\in\mathcal{E}}$ and the states of the fixed leaders $\{p_i^*\}_{i\in\mathcal{V}_l}$ $\Leftrightarrow$ $\mathcal{B}_{ff}$ is full rank.*

For a better understanding of the construction of the desired formation, an illustrative example is provided in Fig. 1, where the leaders are denoted by solid circles and the followers are denoted by hollow circles. The interaction topology shown in Fig. 1 (a) cannot guarantee the uniqueness of the target formation. However, the target formation can be determined uniquely by implementing the interaction topologies in Fig. 1 (b) and (c).

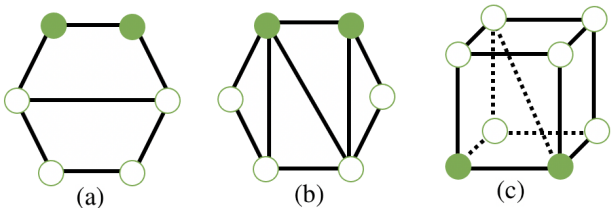

Fig. 1. Examples of non-unique target formation (a) and unique target formation (b and c) determined by bearing vectors.

B. Problem Statements

In this paper, we focus on developing a collaboration protocol for networked agents in the presence of exogenous disturbance. Thus the single-integrator dynamics of the vehicles are considered for simplicity. Suppose the leaders are fixed ($\dot{p}_i = 0$, $\forall i \in \mathcal{V}_l$), and the dynamics of the followers is

$$\dot{p}_i(t) = u_i(t) + \omega_i, \quad i \in \mathcal{V}_f. \tag{2}$$

where $\omega_i \in \mathbb{R}^d$ is the exogenous disturbance of vehicle $i \in \mathcal{V}_f$.

Remark 1. *Although the dynamics of most robotic systems (e.g., wheeled mobile robots and quadrotor UAVs) are nonlinear and coupled, the input–output feedback linearization technique [38] can be exploited to transform the dynamics of the robots to a single-integrator system at any operating point. This technique has been widely applied to mobile robots [39], [40]. Hence, this work particularly focuses on designing control protocols for multi-vehicle formation based on the linearized model with external disturbances.*

Let $\delta_i = p_i - p_i^*$ and $\delta = \mathrm{col}(\delta_1,\cdots,\delta_n)$ denote the formation error, the assumptions are given as follow:

Assumption 1: The exogenous disturbance is upper-bounded i.e., $\|\omega_i\| \leq f_i$, where f_i is a positive constant.

From Assumption 1, we can easily conclude that $\|\omega\| \leq F = \sum_{i=n_{l+1}}^{n} f_i$, where $\omega = \mathrm{col}(\omega_{n_{l+1}},\cdots,\omega_n)$.

Assumption 2: In the single-integrator system with exogenous disturbance, the formation scale $\mathbf{s}(t)$ is upper-bounded from the initial scale. i.e., $\mathbf{s}(t) \leq \mathbf{s}(0) = \mathbf{s}_0$, $\forall\ t \geq 0$.

Assumption 3: The target formation is unique, i.e., $\mathcal{B}_{ff} > 0$.

Assumption 4: There is no collision between each vehicle during the task.

From Assumption 4, we can deduce that there exists $\tau > 0$ such that $\|p_i - p_j\| > \tau$, $\forall i,j \in \mathcal{V}$

We now demonstrate the problem statement of this paper in a precise form. Suppose the dynamics of each mobile vehicle with exogenous disturbances is guaranteed by system (2). To ensure a superior performance of the formation tracking mission, the main objectives can be described as: i) Developing a novel finite-time controller for each vehicle $i \in \mathcal{V}_f$ based on bearing vectors $\{g_{ij}(t)\}_{j\in\mathcal{N}_i}$ and exploring the convergence of the formation error δ. ii) Providing the fault-tolerant analysis of the finite-time protocol in the presence of actuator failures in the hardware. iii) Extending the capacity of the designed controller to deal with LTI systems with exogenous disturbances, which is more general in practical robotic platforms.

III. Main Results

Formation tracking algorithms can be used effectively for swarm robots to converge to the desired pattern in a distributed manner. In this section, we first introduce a finite-time formation control protocol with bearing-only measurements. Then, we provide the stability analysis to guarantee the performance of the formation protocol under external disturbances and actuator faults. Thus it can be implemented safely by practitioners in extreme environments.

A. Controller Design with Exogenous Disturbance

In this section, the robust formation tracking problem with exogenous disturbance and bearing measurements is considered. The coordinated protocol of each follower is designed as

$$u_i(t) = (a + b\frac{\dot{\mu}}{\mu}) \sum_{j\in\mathcal{N}_i} (g_{ij}(t) - g^*_{ij}(t)), \quad i \in \mathcal{V}_f. \tag{3}$$

where $a > 0$ and $b > 0$ are two gains, and $\mu : \mathbb{R}^+ \to \mathbb{R}^+$ is a time-varying scaling function defined as

$$\mu(t) = \begin{cases} \dfrac{T^h}{(T-t)^h} & t \in [0, T) \\ 1, & t \in [T, \infty), \end{cases} \tag{4}$$

where h is a parameter to be specified. By using the right-hand derivative of $\mu(t)$ at $t = T$ as $\dot{\mu}(T)$, we have

$$\dot{\mu}(t) = \begin{cases} \dfrac{h}{T}\mu^{(1+\frac{1}{h})}, & t \in [0, T) \\ 0, & t \in [T, \infty). \end{cases} \tag{5}$$

$\mu(t)$ is important in the controller since it ensures the bearing-only formation task can be finished in finite time T which can be predefined by users.

Since there exists the unknown exogenous disturbances in the system. The goal is to discuss the robustness of the FTBO controller (3). Before we show the main theorem and associate proof, the following lemmas should be introduced

Lemma 2. *[22]: If Assumption 4 holds, we have*

$$p^\top \bar{H}^\top (g^* - g) \le 0 \tag{6}$$

$$(p^*)^\top \bar{H}^\top (g^* - g) \ge 0 \tag{7}$$

$$(p - p^*)^\top \bar{H}^\top (g^* - g) \le 0 \tag{8}$$

Lemma 3. *[22]: If Assumption 4 holds, we have*

$$p^\top \mathcal{B} p \le 2p^\top \bar{H}^\top (g - g^*) \max_k \|e_k\| \tag{9}$$

Lemma 4. *Suppose $z : \mathbb{R} \to \mathbb{R}_{\ge 0}$ is a continuously differentiable function, if*

$$\dot{z}(t) \le -az - b\frac{\dot{\mu}}{\mu} z + \varepsilon, \quad t \in [0, \infty) \tag{10}$$

where a, b, and ε are positive and $bh > 1$. Then, it follows that

$$z(t) \begin{cases} \le \mu^{-b} e^{-at} z(0) + \epsilon(t), & t \in [0, T) \\ \le \varepsilon/a, & t \in [T, \infty) \end{cases} \tag{11}$$

where

$$\epsilon(t) = (\frac{T-t}{bh-1} - \frac{T\mu^{-b}}{bh-1})\varepsilon. \tag{12}$$

Proof. On one hand, if $t \in [0, T)$. Let $h = \mu^b z$, we have

$$\dot{h} = \mu^b \dot{z} + b\mu^{b-1}\dot{\mu} z = \mu^b(\dot{z} + b\frac{\dot{\mu}}{\mu} z). \tag{13}$$

From (10), we can get

$$\begin{aligned} \dot{h} &\le \mu^b(-az + \varepsilon) \\ &= -ah + \mu^b \varepsilon \end{aligned} \tag{14}$$

That is to say

$$\begin{aligned} h &\le e^{-at}(h(0) + \varepsilon \int_0^t \mu^b(\tau) e^{a\tau} d\tau) \\ &\le e^{-at} h(0) + \varepsilon \int_0^t \mu^b(\tau) d\tau \end{aligned} \tag{15}$$

then it can be obtained that

$$\begin{aligned} z &\le \mu^{-b}(e^{-at} z(0) + \varepsilon \int_0^t \mu^b(\tau) d\tau) \\ &\le \mu^{-b}(e^{-at} z(0) + (\frac{T^{bh}}{(bh-1)(T-t)^{bh-1}} \\ &- \frac{T}{bh-1})\varepsilon) \\ &= \mu^{-b} e^{-at} z(0) + \epsilon(t). \end{aligned} \tag{16}$$

On the other hand, if $t \in [T, +\infty)$, we have

$$\dot{z} \le -az + \varepsilon \tag{17}$$

Hence, we can conclude that $z \le \varepsilon/a$. This completes the proof. □

Lemma 5. *if a and b are two unit vectors. Let $\alpha \ge \beta \ge 0$, then*

$$\|\alpha a - \beta b\| \ge \beta \|a - b\|.$$

Proof. It can be easily found that

$$\begin{aligned} \|\alpha a - \beta b\|^2 - (\beta\|a - b\|)^2 &= \alpha^2 - \beta^2 - 2\alpha\beta\cos\phi + 2\beta^2\cos\phi \\ &= (\alpha - \beta)(\alpha + \beta - 2\beta\cos\phi) \\ &\ge 2\beta(\alpha - \beta)(1 - \cos\phi) \\ &\ge 0, \end{aligned}$$

where ϕ is angle between a and b. We finish the proof. □

Now, we would like to give the following analysis of the robustness of the multi-vehicle network under the proposed control protocol.

Theorem 1. *Consider the single-integrator system with the exogenous disturbance. Under Assumption 1-4 and protocol (3), let $K = 2ns_0$, by choosing $\gamma = \sqrt{K/a\lambda_{min}(\mathcal{B}_{ff})}$ and*

$$bh\lambda_{min}(\mathcal{B}_{ff}) > 2K, \tag{18}$$

the formation error δ converges to the bound set $\mathcal{S}$

$$\mathcal{S} = \left\{ \delta : \|\delta\|^2 \le \frac{4\gamma^2 F^2 K}{a\lambda_{\min}(\mathcal{B}_{ff})} \right\}.$$

in finite time. Furthermore, the control input u is C^1 smooth and uniformly bounded over the time interval $[0,\infty)$.

Proof. By implementing the protocol (3), the dynamics of (2) can be written in a compact form as

$$\dot{p} = (a + b\frac{\dot{\mu}}{\mu}) \begin{bmatrix} 0 & 0 \\ 0 & I_{dn_f} \end{bmatrix} \bar{H}^\top (g^* - g) + \omega. \tag{19}$$

The Lyapunov function can be constructed as $V = \frac{1}{2}\|\delta\|^2$. The derivative of V can be described as

$$\begin{aligned} \dot{V} &= \delta^\top \dot{p} \\ &= (a + b\frac{\dot{\mu}}{\mu})\delta^\top \begin{bmatrix} 0 & 0 \\ 0 & I_{dn_f} \end{bmatrix} \bar{H}^\top (g^* - g) + \delta^\top \omega \\ &= (a + b\frac{\dot{\mu}}{\mu})\delta^\top \bar{H}^\top (g^* - g) + \delta^\top \omega \\ &= (a + b\frac{\dot{\mu}}{\mu})(p - p^*)^\top \bar{H}^\top (g^* - g) + \delta^\top \omega. \end{aligned} \tag{20}$$

From Lemma 2 and 3, we can substitute (9) in (20). Since $\mathcal{B}p^* = 0$ and $\delta = [0, \delta_f^\top]$, we have

$$\begin{aligned} \dot{V} &= (a + b\frac{\dot{\mu}}{\mu})(p - p^*)^\top H^\top (g^* - g) + \delta^\top \omega \\ &\le (a + b\frac{\dot{\mu}}{\mu}) p^\top H^\top (g^* - g) + \delta^\top \omega \\ &\le -(a + b\frac{\dot{\mu}}{\mu}) \frac{1}{2\max_k \|e_k\|} p^\top \mathcal{B} p + \delta^\top \omega \\ &\le -(a + b\frac{\dot{\mu}}{\mu}) \frac{\lambda_{\min}(\mathcal{B}_{ff})}{2\max_k \|e_k\|} \|\delta\|^2 + \delta^\top \omega. \end{aligned} \tag{21}$$

For all vehicles in the system, from Cauchy inequality, we have

$$\begin{aligned} n^2 \mathbf{s}(t)^2 &= n \sum_{k=1}^{n} \|p_k - \bar{p}\|^2 \\ &\ge (\|p_i - \bar{p}\| + \sum_{k \in \mathcal{V}, k \ne i}^{n} \|p_k - \bar{p}\|)^2 \\ &\ge \|p_i - \bar{p}\|^2 \end{aligned} \tag{22}$$

From (22) and Assumption 2, we can obtain

$$\begin{aligned} \|e_k\| &= \|p_i - p_j\| \\ &= \|(p_i - \bar{p}) - (p_j - \bar{p})\| \\ &\le \|p_i - \bar{p}\| + \|p_j - \bar{p}\| \\ &\le 2n\mathbf{s}(t) \le 2n\mathbf{s}_0 = K. \end{aligned} \tag{23}$$

By average inequality, we have

$$\frac{\gamma^{-2}}{4}\|\delta\|^2 + \gamma^2 \|\omega\|^2 \ge \|\delta^T\| \|\omega\| \ge \delta^T \omega. \tag{24}$$

Combine with (23), (21) can be written as

$$\begin{aligned} \dot{V} &\le -(a + b\frac{\dot{\mu}}{\mu}) \frac{\lambda_{\min}(\mathcal{B}_{ff})}{2K} \|\delta\|^2 + \delta^\top \omega \\ &\le -(a + b\frac{\dot{\mu}}{\mu})(\frac{\lambda_{\min}(\mathcal{B}_{ff})}{2K} \|\delta\|^2) + \frac{\gamma^{-2}}{4}\|\delta\|^2 + \gamma^2 \|\omega\|^2 \\ &\le -(a + b\frac{\dot{\mu}}{\mu})(\frac{\lambda_{\min}(\mathcal{B}_{ff})}{2K} - \frac{\gamma^{-2}}{4a}) \|\delta\|^2 + \gamma^2 \|\omega\|^2 \end{aligned} \tag{25}$$

By choosing

$$\gamma = \sqrt{\frac{K}{a\lambda_{\min}(\mathcal{B}_{ff})}} \tag{26}$$

and following Assumption 1, we have

$$\dot{V} \le -(a + b\frac{\dot{\mu}}{\mu}) \frac{\lambda_{\min}(\mathcal{B}_{ff})}{4K} V + \gamma^2 F^2. \tag{27}$$

Therefore

$$\begin{aligned} \dot{V} &\le -\frac{a\lambda_{\min}(\mathcal{B}_{ff})}{2K} V - \frac{b\lambda_{\min}(\mathcal{B}_{ff})}{2K} \frac{\dot{\mu}}{\mu} V + \gamma^2 F^2 \\ &= -\bar{a} V - \bar{b}\frac{\dot{\mu}}{\mu} V + \gamma^2 F^2, \end{aligned} \tag{28}$$

where $\bar{a} = \frac{a\lambda_{\min}(\mathcal{B}_{ff})}{2K}$ and $\bar{b} = \frac{b\lambda_{\min}(\mathcal{B}_{ff})}{2K}$.

In light of Lemma 4, we have

$$\|\delta(t)\|^2 \begin{cases} \le \mu^{-\bar{b}} e^{-\bar{a}t} \|\delta(0)\|^2 + 2\bar{\epsilon}(t), & t \in [0, T) \\ \le 2\gamma^2 F^2 / \bar{a}, & t \in [T, \infty) \end{cases} \tag{29}$$

where

$$\bar{\epsilon}(t) = (\frac{T - t}{\bar{b}h - 1} - \frac{T\mu^{-\bar{b}}}{\bar{b}h - 1})\gamma^2 F^2. \tag{30}$$

Since

$$\lim_{t \to T^-} \mu^{-\bar{b}} = 0, \tag{31}$$

it is easily to get

$$\lim_{t \to T^-} \bar{\epsilon}(t) = 0. \tag{32}$$

From (31) and (32), it can be concluded that

$$\lim_{t \to T^-} \|\delta(t)\| = 0. \tag{33}$$

Hence, we can obtain that the formation error δ converge to the bound set $\mathcal{S}$ in finite time T from Lemma 4.

Next, we will discuss the continuity and boundary of u and du/dt. By (19), we have

$$\|u\| \le (a + b\frac{\dot{\mu}}{\mu}) \|\bar{H}^\top\| \|(g - g^*)\|. \tag{34}$$

By Lemma 5 and Assumption 4, we obtain

$$\begin{aligned} \|e - e^*\| &= \sqrt{\sum_{i=1}^{m} \|g_i\|e_i\| - g_i^*\|e_i^*\|\|^2} \\ &\ge \sqrt{\tau \sum_{i=1}^{m} \|g_i - g_i^*\|^2} \\ &\ge \sqrt{m\tau}\|g - g^*\|, \end{aligned} \tag{35}$$

then it follows

$$\|g - g^*\| \le \frac{1}{\sqrt{m\tau}}\|e - e^*\| \le \frac{1}{\sqrt{m\tau}} \|\bar{H}\| \|\delta(t)\|. \tag{36}$$

Combine (29) with (34), we have u is bounded if $t \ge T$ and

$$\|u\| \le \frac{\mu^{-(\bar{b} - \frac{1}{h})} e^{-\bar{a}t} \|\bar{H}^\top\| \|\bar{H}\| \|\delta(0)\|}{T\sqrt{m\tau}} (Ta\mu^{-\frac{1}{h}} + bh). \tag{37}$$

From (18), we have $\bar{b} - \frac{1}{h} > 0$. Combined with (29), (34),

(37), we can conclude that

$$\lim_{t\to T^-}\|u\|=0. \tag{38}$$

Hence, we finish the proof of the continuity and uniformly boundness of u on $[0,\infty)$.

Next, we will focus on du/dt. We have

$$\begin{aligned}\frac{du}{dt}=&\frac{bh}{T^2}\mu^{\frac{2}{h}}\bar{H}^\top(g-g^*)+(a+b\frac{\dot{\mu}}{\mu})\bar{H}^\top\dot{g}\\ =&\frac{bh}{T^2}\mu^{\frac{2}{h}}\bar{H}^\top(g-g^*)\\ &+(a+b\frac{\dot{\mu}}{\mu})\bar{H}^\top\text{diag}(\frac{P_{g_k}}{\|e_k\|})\bar{H}\dot{p}\\ =&\frac{bh}{T^2}\mu^{\frac{2}{h}}\bar{H}^\top(g-g^*)\\ &+(a+b\frac{\dot{\mu}}{\mu})^2\bar{H}^\top\text{diag}(\frac{P_{g_k}}{\|e_k\|})\bar{H}\bar{H}^\top(g-g^*).\end{aligned} \tag{39}$$

It is easy to see that the continuity of (du/dt) can be guaranteed on $[0,T)$ and (T,∞) and$\|\text{diag}(\frac{P_{g_k}}{\|e_k\|})\|$ is bounded. Hence, there is a matrix $\Lambda>0$ such that $\|\bar{H}^\top\|^2\|\bar{H}\|\|\text{diag}(\frac{P_{g_k}}{\|e_k\|})\|<\Lambda$. According to (39), we can obtain

$$\begin{aligned}\left\|\frac{du}{dt}\right\|=&\|\bar{H}^\top\|^2\|\bar{H}\|\|\text{diag}(\frac{P_{g_k}}{\|e_k\|})\|(a+b\frac{\dot{\mu}}{\mu})^2\|g-g^*\|\\ &+\frac{bh}{T^2}\mu^{\frac{2}{h}}\|\bar{H}^\top\|\|g-g^*\|\\ &\le[\Lambda a^2+2ab\Lambda\mu^{\frac{1}{h}}+(\Lambda b^2+\frac{bh}{T^2}\|\bar{H}^\top\|)\mu^{\frac{2}{h}}]\|g-g^*\|.\end{aligned} \tag{40}$$

Based on (18), we can get $\bar{b}-\frac{2}{h}>0$. Similar to analysis for $\|u\|$ in (37) and (40), we have

$$\lim_{t\to T^-}\|\frac{du}{dt}\|=0. \tag{41}$$

Hence, the continuity and uniformly boundness of du/dt can also be guaranteed on $[0,\infty)$. Hence we complete the proof. □

Remark 2. *The time-varying gain $\frac{\dot{\mu}}{\mu}$ affects the tracking performance of the controller. From* (37) *and* (40)*, we discuss the relationship between $\|u\|$ and $\|\delta\|$, and then imply that the continuity and uniformly boundness of the control input u can be guaranteed by* (18)*. That is to say, the decrease of $\|\delta\|$ is faster than the increase of $\frac{\dot{\mu}}{\mu}$ if b and h are big enough. Furthermore, the scaling function in* (4) *is designed to guarantee the finite-time convergence of the controller. Since there is no fractional power feedback or signum functions in the proposed controller (different from [26], [34], [35]), the control input remains C^1 smooth. Besides, the desired settling time is not related to the initial states and thus can be predefined by users.*

Following the analysis presented above, the procedure to construct the protocol u_i is given in Algorithm 1.

Algorithm 1 Finite-time bearing-only protocol design

1: Select n_l leader vehicles and n_f follower vehicles;
2: Set the target formation configuration p^* and compute the target bearing g^*;
3: Set the initial positions for fixed leaders and followers
4: Set the bidirectional communication graph and the oriented graph among each vehicle;
5: **if** Assumption 4 is satisfied **then**
6: Compute the edge vectors and bearing vectors for each connected vehicle;
7: Compute the bearing Laplacian matrix $\mathcal{B}$ as shown in (1);
8: **if** $\mathcal{B}_{ff}>0$ **then**
9: Set the finite time T;
10: Select the positive control parameters a, b, and h;
11: **if** condition (18) holds **then**
12: Construct the control law u_i given in (3);
13: **else**
14: Back to step 9;
15: **end if**
16: **else**
17: Back to step 4;
18: **end if**
19: **else**
20: Back to step 3;
21: **end if**

B. Fault-Tolerant Analysis

Based on the fact that actuator failures (e.g., the efficiency and the output bias) of the controller could not be ignored in some platforms. The fault-tolerant analysis of the proposed controller is discussed in this subsection. We explore the robustness of the controller (3) with the exogenous disturbances and the actuator failures.

The actuator failures u_i^f of each follower agent can be expressed as

$$u_i^f(t)=\rho_i(t)u_i(t)+\tilde{b}_i(t), \tag{42}$$

where $\rho_i(t)\in(0,1]$ represents the unknown efficiency factor of the actuator channel, and $\tilde{b}_i(t)=[\tilde{b}_{i1}(t),\cdots,\tilde{b}_{id}(t)]^\top$ represents the unknown output bias of the actuator channel following [14], [17], [41]. For both time-varying $\rho_i(t)$ and $\tilde{b}_i(t)$, we have the following assumption

Assumption 5: The unknown efficiency factor and unknown output bias are bounded, and there exists a positive constant $\rho*$ and $\tilde{b}^*$ such that $0<\rho^*\le\rho_i(t)\le 1$ and $\|b_i(t)\|\le\tilde{b}_i^*$.

From Assumption 5, we can easily conclude that $\|\tilde{b}(t)\|\le\tilde{b}^*=\sum_{i=n_{l+1}}^{n}\tilde{b}_i^*$, where $\tilde{b}(t)=\text{col}(\tilde{b}_{n_{l+1}}(t),\cdots,\tilde{b}_n(t))$.

Suppose the leaders are fixed, the dynamics of the followers can be described as

$$\dot{p}_i(t)=u_i^f(t)+\omega_i\quad i\in\mathcal{V}_f. \tag{43}$$

Now, we would like to present the following result of the fault-tolerant analysis of the multi-vehicle network under the proposed control protocol.

Theorem 2. *Consider the single-integrator system with the exogenous disturbance and actuator failures. Under Assumption 1-5, let $K=2ns_0$, by choosing $\gamma=\sqrt{K/\rho^*a\lambda_{min}(\mathcal{B}_{ff})}$*

and

$$\rho^* bh\lambda_{min}(\mathcal{B}_{ff}) > 2K, \tag{44}$$

the formation error δ converges to the bound set $\mathcal{S}$

$$\mathcal{S} = \left\{ \delta : \|\delta\|^2 \leq \frac{4\gamma^2(F+\tilde{b}^*)^2K}{\rho^* a\lambda_{\min}(\mathcal{B}_{ff})} \right\}.$$

in a finite time.

Proof. By implementing the protocol (3), the compact form of (2) can be written as

$$\dot{p} = (a + b\frac{\dot{\mu}}{\mu}) \begin{bmatrix} 0 & 0 \\ 0 & \bar{\rho}(t) \end{bmatrix} \bar{H}^\top (g^* - g) + \omega + \tilde{b}(t). \tag{45}$$

Choosing Lyapunov function as $V = \frac{1}{2}\|\delta\|^2$. The derivative of V can be described as

$$\begin{aligned} \dot{V} &= \delta^\top \dot{p} \\ &= (a + b\frac{\dot{\mu}}{\mu})\delta^\top \begin{bmatrix} 0 & 0 \\ 0 & \bar{\rho}(t) \end{bmatrix} \bar{H}^\top (g^* - g) + \delta^\top(\omega + \tilde{b}(t)) \\ &\leq (a + b\frac{\dot{\mu}}{\mu})\rho^*(p - p^*)^\top \bar{H}^\top (g^* - g) + \delta^\top(\omega + \tilde{b}(t)). \end{aligned} \tag{46}$$

The last inequality can be obtained by Assumption 5. By average inequality, we have

$$\begin{aligned} \delta^\top(\omega + \tilde{b}(t)) &\leq \|\delta^\top\|(\|\omega\| + \|\tilde{b}(t)\|) \\ &\leq \|\delta^\top\|(\|\omega\| + \tilde{b}^*) \\ &\leq \frac{\gamma^{-2}}{4}\|\delta\|^2 + \gamma^2(\|\omega\| + \tilde{b}^*)^2 \end{aligned} \tag{47}$$

Choosing

$$\gamma = \sqrt{\frac{K}{\rho^* a\lambda_{\min}(\mathcal{B}_{ff})}} \tag{48}$$

According to (21)-(23), (25), and (27), we can get

$$\begin{aligned} \dot{V} \leq& -\frac{\rho^* a\lambda_{\min}(\mathcal{B}_{ff})}{2K}V - \frac{\rho * b\lambda_{\min}(\mathcal{B}_{ff})}{2K}\frac{\dot{\mu}}{\mu}V \\ &+ \gamma^2(F+\tilde{b}^*)^2 \\ =& -a_f V - b_f\frac{\dot{\mu}}{\mu}V + \gamma^2(F+\tilde{b}^*)^2 \end{aligned} \tag{49}$$

with $a_f = \frac{\rho^* a\lambda_{\min}(\mathcal{B}_{ff})}{2K}$ and $b_f = \frac{\rho^* b\lambda_{\min}(\mathcal{B}_{ff})}{2K}$.

From Lemma 4, we have

$$\|\delta(t)\|^2 \begin{cases} \leq \mu^{b_f} e^{-a_f t}\|\delta(0)\|^2 + 2\epsilon_f(t), & t \in [0, T) \\ \leq 2\gamma^2(F+\tilde{b}^*)^2/a_f, & t \in [T, \infty) \end{cases} \tag{50}$$

where

$$\epsilon_f(t) = (\frac{T-t}{b_f h - 1} - \frac{T\mu^{-b_f}}{b_f h - 1})\gamma^2(F+\tilde{b}^*)^2. \tag{51}$$

Similar to the analysis in Theorem 1, we can find that the formation error δ converge to the bound set $\mathcal{S}$ in finite time T from Lemma 4. This completes the proof. □

Remark 3. *The performance of the finite-time controller is affected by the efficiency factor and the output bias of the actuator channel. The formation error is closer to zero for smaller output bias and larger control gain a, which can reduce the effect of the actuator failures. From* (50)*, it can be obtained that the decrease of $\|\delta\|$ is faster for larger a_f, b_f, and ρ^*. Hence, the convergence rate of the formation error is determined by the boundary of the efficiency factor.*

C. Extension to the LTI Systems with Exogenous Disturbance

Considering that some robotic platforms may have general linear dynamics (e.g., after implementing geometry-based robust feedback linearization techniques), in this subsection, we aim to extend the results obtained from the previous subsections to solve the robust formation coordination problem with exogenous disturbance and bearing measurement for LTI systems.

Suppose the leaders are fixed ($\dot{p}_i = 0$, $\forall i \in \mathcal{V}_l$), and the dynamics of the followers can be described by

$$\dot{p}_i(t) = A_i p_i + u_i(t) + \omega_i, \quad i \in \mathcal{V}_f, \tag{52}$$

where $A_i \in \mathbb{R}^{d\times d}$, and $\omega_i \in \mathbb{R}^d$ is the exogenous disturbance of vehicle $i \in \mathcal{V}_f$.

Under the protocol (3), the dynamic of (52) can be written in compact form as

$$\dot{p} = \begin{bmatrix} 0 & 0 \\ 0 & A \end{bmatrix} p + (a + b\frac{\dot{\mu}}{\mu}) \begin{bmatrix} 0 & 0 \\ 0 & I_{dn_f} \end{bmatrix} \bar{H}^\top (g^* - g) + \omega, \tag{53}$$

where $A = \text{diag}\{A_{n_l+1}, \cdots, A_n\} \in \mathbb{R}^{n_f\times n_f}$.

Let $p = [p_l^\top, p_f^\top]^\top$, where $p_l = \text{col}(p_1, \cdots, p_{n_l})$ and $p_f = \text{col}(p_{n_l+1}, \cdots, p_n)$ denote the positions of leaders and followers. We have the following corollary.

Corollary 1. *Consider the LTI system with the exogenous disturbance. Under Assumption 1-4, if A_i is negative semi-definite, and ${p_i^*}^\top A_i = 0$ for each follower vehicle $i \in \mathcal{V}_f$, the formation error δ converge to the bound set $\mathcal{S}$*

$$\mathcal{S} = \left\{ \delta : \|\delta\|^2 \leq \frac{4\gamma^2F^2K}{a\lambda_{\min}(\mathcal{B}_{ff})} \right\}.$$

in finite time by protocol (3)*, where $K = 2n\boldsymbol{s}_0$, and $\gamma \geq \sqrt{aK/\lambda_{min}(\mathcal{B}_{ff})}$.*

Proof. The Lyapunov function can be constructed as $V = \frac{1}{2}\|\delta\|^2$. The derivative of V can be expressed as

$$\begin{aligned} \dot{V} =& \delta^\top \dot{p} \\ =& -(a + b\frac{\dot{\mu}}{\mu})(p-p^*)^\top \bar{H}^\top (g - g^*) + \delta^\top \omega \\ &+ (p-p^*)^\top \begin{bmatrix} 0 & 0 \\ 0 & A \end{bmatrix} p. \end{aligned} \tag{54}$$

From (21), since A_i is negative semi-definite and ${p_i^*}^\top A_i = 0$ for each follower vehicle $i \in \mathcal{V}_f$, we have

$$\begin{aligned} \dot{V} \leq& -(a + b\frac{\dot{\mu}}{\mu})\frac{\lambda_{\min}(\mathcal{B}_{ff})}{2\max_k\|e_k\|}\|\delta\|^2 + \delta^\top\omega + \sum_{i=n_l+1}^{n} {p_i^*}^\top A_i p_i \\ &+ p_f^\top A p_f \\ \leq& -(a + b\frac{\dot{\mu}}{\mu})\frac{\lambda_{\min}(\mathcal{B}_{ff})}{2\max_k\|e_k\|}\|\delta\|^2 + \delta^\top\omega. \end{aligned} \tag{55}$$

Following similar steps in Theorem 1, we can imply that the formation error δ converge to the bound set $\mathcal{S}$ in finite time by protocol (3). This completes the proof. □

IV. Simulation and Experimental Results

To verify the effectiveness of the obtained results, Matlab simulation results and hardware experimental results using real mobile robots are shown in this section.

A. Formation Tracking Control Performance

We design the simulations to validate the effectiveness and the continuous of the FTBO controller with exogenous disturbance. Five UAVs, with two leaders and three followers, are used in this task. These UAVs aim to attain a pentagon shape desired formation in a 3D space via bearing-only measurements in the presence of unknown exogenous disturbances with the boundary 0.1. For the controller design, we choose the parameters as $a = 2$, $b = 8$, $h = 5$, and $T = 50$ s.

By implementing Algorithm 1, the trajectories of the UAVs during the formation forming mission are shown in Fig. 2. The positions of the two fixed leaders (marked by blue and green squares) in the x-y-z plane are selected as $(2.5, 2, 0)$ and $(2.5, 5, 0)$, respectively. The initial positions of three followers are selected as $(2, 6, 4)$, $(4, 1, 3)$, and $(1, 3, 0.5)$ respectively. The interaction topology between each agent is represented by red solid lines. We adopt the yellow, pink, and dark green dotted lines to denote the movements of the followers from $t = 0$ s to $t = 50$ s. The formations of the UAVs are captured at time instants $t = 0$ s, $t = 5$ s $t = 15$ s, and $t = 50$ s (From $(a) - (d)$ in Fig. 2), respectively. Fig. 3(a) shows the control actions of the followers during the mission. From the curves of the control inputs, it can be concluded that the controller can converge to zero in finite-time smoothly. Fig. 3(b) reveals that $\|\delta\|$ (represented by blue solid line) will converge to a bound set at $t = 50$ s. The tracking errors of three followers are denoted by the yellow, pink, and dark green dash lines. As can be seen from all these figures, the bearing-only formation tracking task has been accomplished by the proposed finite-time protocol under unknown external disturbances.

B. Fault-Tolerant Formation Tracking with Different Parameters

In this section, four simulation case studies (with different efficiency factors and output bias) are conducted to explore the relationship between the fault parameters and the performances of the controller in the presence of the exogenous disturbance. The selection of ρ^* and $\bar{b}^*$ is presented in TABLE I. $\rho_i(t)$ and $\tilde{b}_i(t)$ are generated randomly at any time t to satisfy Assumption 5 for each vehicle to simulate the unknown actuator failures. Twelve UAVs, with three leaders and nine followers, are used to complete the formation task within the finite-time $T = 50$ s. The interaction topology between these UAVs is shown in Fig. 4. These UAVs aim to attain the desired formation as two equilateral triangles in a 2D space via bearing-only measurements in the presence of unknown exogenous disturbances with boundary 0.1.

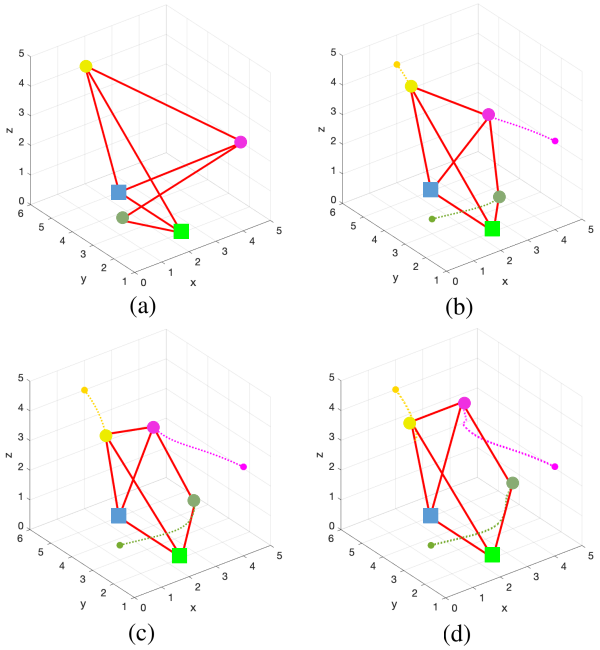

Fig. 2. Trajectories of the networked UAVs at different time instants during the formation forming mission. (a) $t = 0$ s; (b) $t = 5$ s; (c)$t = 15$ s and (d) $t = 50$ s.

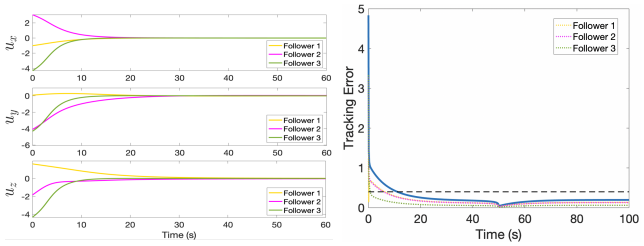

Fig. 3. (a) Control actions of the follower UAVs along the X-axis, Y-axis and Z-axis and (b) Time variation of the formation tracking error. The black dash line denotes the computed bound.

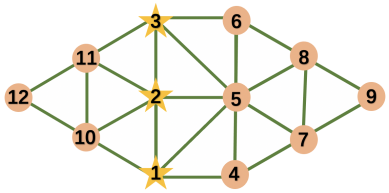

Fig. 4. Interaction topology between each UAV.

In order to satisfy the conditions in Theorem 2, we set the parameters as $a = 2$, $b = 8$, and $h = 5$ for all the examples. By implementing the controller to (43), the trajectories and the tracking errors of the mobile robots during the formation forming mission are shown in Fig. 5 and Fig. 6 ($(a) - (d)$ represent the example 1-4). The positions of the three fixed leaders (marked by three yellow stars) are selected as $(-2, 0)$, $(0, 0)$, and $(2, 0)$, respectively. We select the same initial positions of the nine followers for all the examples. It can be concluded from (a), (b), and (d) in Fig. 5 that different

TABLE I
SELECTION OF ρ^* AND $\bar{b}^*$

	ρ^*	$\bar{b}^*$
Example 1	0.8	0.05
Example 2	0.5	0.05
Example 3	0.5	0.2
Example 4	0.3	0.05

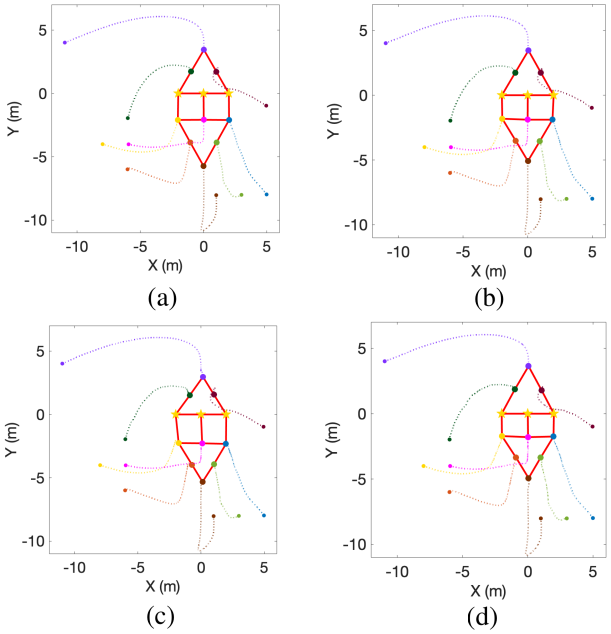

Fig. 5. Trajectories of the followers for Example 1 (a), Example 2 (b), Example 3 (c), and Example 4 (d).

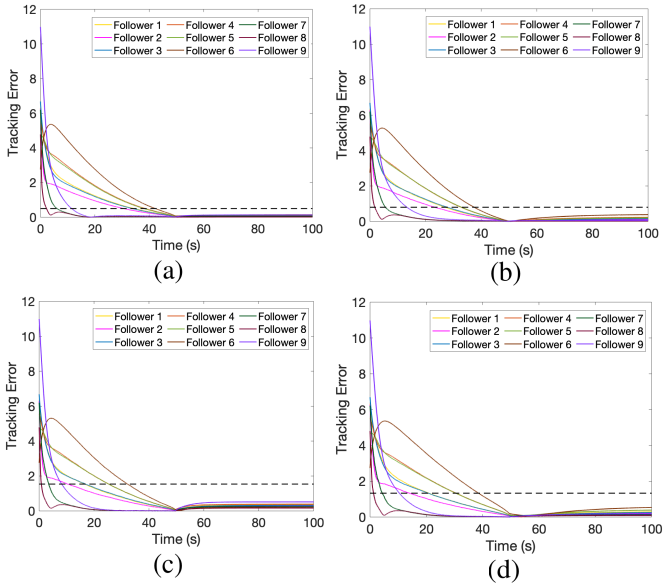

Fig. 6. Tracking error of the followers for Example 1 (a), Example 2 (b), Example 3 (c), and Example 4 (d). The black dash line denotes the computed bound for each example.

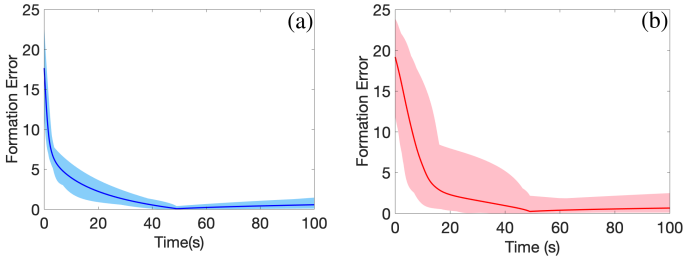

Fig. 7. The performance of (a) the proposed controller and (b) the conventional method proposed in [23].

efficiency factors (ρ^*) affect the performance slightly if the parameters a, b, and h are chosen appropriately to satisfy the conditions in Theorem 2. We can also obtain that different efficiency factors can affect the convergence rate of some followers from (a), (b), and (d) in Fig. 6. From (b) and (c) in Fig. 5 and Fig. 6, we can conclude that the bound set $\mathcal{S}$ is expanded for large output bias ($\bar{b}^*$). Hence, the tracking error will increase, and the final formation shape will be affected in a certain degree for large output bias. From all these figures and analyses, it can be concluded that the bearing-only fault-tolerant formation tracking task has been accomplished by the proposed finite-time protocol under unknown external disturbances.

C. Comparison and Discussion

In recent years, some bearing-based formation control methods have been developed in the literature. In [26], [34], [35], the signum functions were used in the designed protocols to ensure finite-time convergence. However, the controller becomes non-smooth, and the settling time depends on the initial state. To overcome this limitation, an improved bearing-based finite-time controller for double-integrator was considered in a recent work [42]. However, the position measurements are still required in the proposed algorithm, which increases the sensing requirements in the hardware implementation. Compared with those aforementioned works related to bearing-based control protocol design, the proposed FTBO protocol also facilitates robustness against exogenous disturbance and actuator faults.

To highlight the superior robust performance of the FTBO protocol proposed in this paper, we make a comparison between the proposed controller and the conventional bearing-only method proposed in [23], which adopts the same scaling function $\mu(t)$ with different forms of the bearing-based scheme. According to the conventional results, the convergence rate of the traditional method relies on the initial formation error, which is possible to affect the performance of the controller under the exogenous disturbance and actuator failures. In this comparison, four UAVs, with two leaders and two followers, are used to attain the desired square formation via bearing-only measurements in the presence of unknown exogenous disturbances with the boundary 0.05. The boundary of the efficiency factor (ρ^*) and the output bias ($\bar{b}^*$) are chosen as 0.3 and 0.05. For each controller design, we choose the same interaction topology and the same parameters as shown in Section A. The initial states of the leaders are set as $[0, 0]$

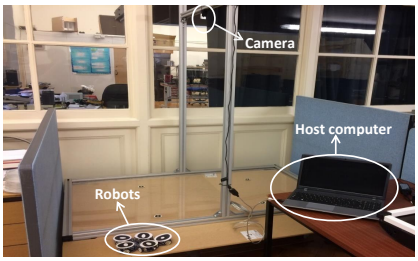

Fig. 8. The experimental arena includes the overhead camera tracking system, the base station and the small-scale mobile vehicles.

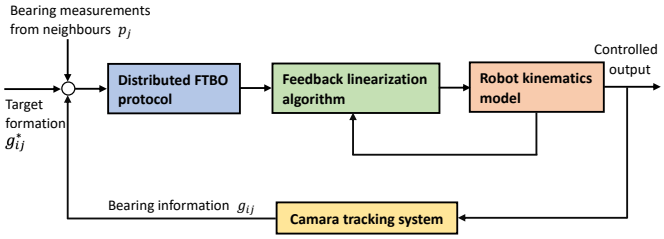

Fig. 9. The hardware control loop of the experiment.

and $[6, 0]$. The initial states of the followers are selected randomly from $[1, 11] \times [1, 11]$. 50 simulations are run for both controllers.

The performances of the proposed protocol and the conventional bearing-only protocol are demonstrated in Fig. $7(a)$ and (b), respectively. The formation error is defined as $\|p - p^*\|$. The blue and red zones display the 50 times simulation results of the protocols proposed in this paper and the conventional strategy, and the blue and red solid lines represent the average values. It can be obtained that the formation error of the proposed protocol can converge to a small bound set under the exogenous disturbance and actuator faults with any initial state of the followers. However, under the conventional method, the formation tracking error becomes large if the initial positions of the followers are far away from the leaders. Hence, compared to the conventional controller, the proposed approach shows a better robust performance against the exogenous disturbances.

D. Experimental Validation

In this section, we conduct lab-based experiments to further verify the feasibility of the proposed method in real-world applications.

For the validation purpose, we use wheeled mobile vehicle Mona [43] as the robotic platform. As shown in Fig. 8, the experimental platform includes a rectangular arena, a digital camera, and a laptop that operates the proposed control algorithm. The control loop of hardware is shown in Fig. 9. For each mobile vehicle, the attached RF (Radio Frequency) module is used to achieve inter-vehicle communication. Also, the feedback linearization algorithm [38] is adopted to transfer the robot kinematics model to a single-integrator system. The relative bearing between the neighbors is detected by the camera tracking system [44] and then transmitted to the formation controller via the ROS (Robot Operating System)

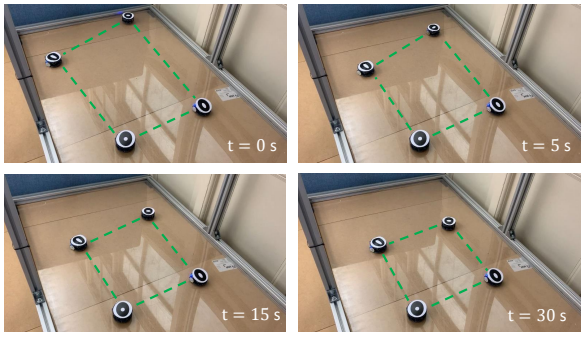

Fig. 10. Progress of the formation tracking task being achieved by a group of four unmanned ground vehicles.

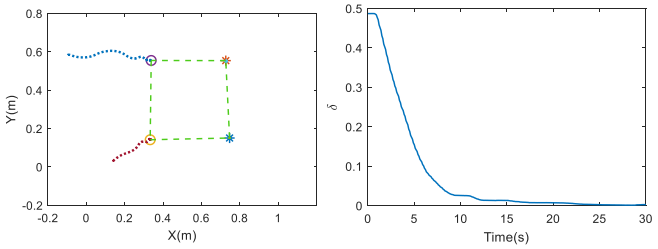

(a) (b)

Fig. 11. (a) Trajectories of the robots in the experiment and (b) time variation of the formation tracking error.

communication framework. Then, the proposed distributed FTBO formation protocol is implemented in each mobile vehicle as the control input.

In the experiment, four mobile vehicles (including two leaders and two followers) aim to achieve a square formation in a given 2D arena. We choose $T = 30$ s as the desired settling time. In the beginning, the four vehicles were randomly placed in the arena. The positions of the mobile vehicles during the experiment are shown in Fig. 10. The trajectories and the formation tracking error are given in Fig. 11(a) and Fig. 11(b), respectively. We emphasize that although the camera tracking system may provide centralized measurements to all the robots, in view of a distributed implementation, each robot only used relative information from its neighbors. The experimental results verified that the designed coordination strategy fulfils the desired objectives in the presence of certain real disturbances such as communication delays and actuator noises.

To further explore the robustness of the FTBO algorithm when the leaders are not fixed, we execute a case study with four mobile vehicle followers and two virtual moving leaders in a 2D space. The trajectories of the virtual leaders are designed as

$$\dot{p}_i = \begin{bmatrix} \dot{p}_{ix}(t) \\ \dot{p}_{iy}(t) \end{bmatrix} = \begin{bmatrix} 0.02 \\ 0.02sin(\frac{4\pi}{65}t) \end{bmatrix}, \quad i \in \mathcal{V}_l, \qquad (56)$$

where $\mathcal{V}_l = \{1, 2\}$. We set the target formation of the followers as a square by bearing-only measurements in the presence of unknown exogenous disturbances with the boundary 0.06. The efficiency factor (ρ^*) and the output bias ($\bar{b}^*$) are selected as 0.5 and 0.05, and the parameters in the controller are chosen

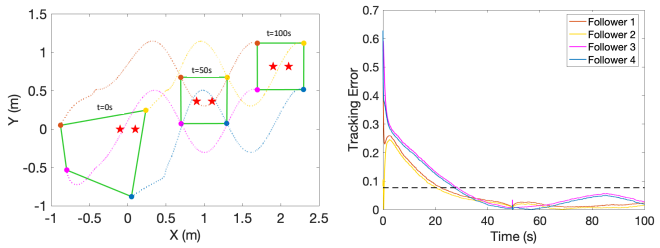

(a) (b)

Fig. 12. (a) The trajectories and (b) the formation tracking errors of the followers with moving leaders.

as: $a = 5$, $b = 5$, and $h = 4$. The formation task is expected to be completed within the finite-time $T = 50$ s.

The movements of the followers under the proposed protocol with moving leaders are illustrated in Fig. 12(a). The initial position of each vehicle is labelled by $t = 0$ s in Fig. 12(a), where the leaders are marked as two red stars. We use the dash curves with four different colors to denote the trajectories of four followers from 0 s to 100 s. Fig. 12(b) displays that the tracking error of each follower during the formation task will converge to a bounded set in the finite-time. Hence, it can be obtained that the followers can converge to the target formation within a finite-time (labelled by $t = 50$ s in Fig. 12(a)) when tracking the movements of the dynamic leaders, which validates the effectiveness of the proposed control design. It can be found that there exists a jump in the tracking error at $t = 50$ s, which is caused by the switching gain in the controller under the effect of the dynamic leaders.

V. Conclusion

In this paper, the finite-time formation tracking problem with bearing-only measurements was addressed. A novel gradient-decent control protocol was proposed to let the multi-vehicle system achieve the target formation through measuring relative bearings of their neighbors. Furthermore, the finite convergence time of the multi-vehicle network with exogenous disturbance was discussed and extended to LTI system. Fault-tolerant analysis was also considered for these vehicles during the formation task. It was validated that the bound of the formation error could be guaranteed when there were external disturbances and actuator failure in the vehicle dynamics. Finally, numerical simulations and practical experiments were provided to verify the obtained results. In the future, the time delay and nonlinear dynamics will be considered in the coordination protocol design.

References

[1] W. Liu, H. Niu, I. Jang, G. Herrmann, and J. Carrasco, "Distributed neural networks training for robotic manipulation with consensus algorithm," *IEEE Transactions on Neural Networks and Learning Systems*, 2022.

[2] H. Bai and J. T. Wen, "Cooperative load transport: A formation-control perspective," *IEEE Transactions on Robotics*, vol. 26, no. 4, pp. 742–750, 2010.

[3] J. Hu, P. Bhowmick, I. Jang, F. Arvin, and A. Lanzon, "A decentralized cluster formation containment framework for multirobot systems," *IEEE Transactions on Robotics*, vol. 37, no. 6, pp. 1936–1955, 2021.

[4] N. Geng, Q. Meng, D. Gong, and P. W. Chung, "How good are distributed allocation algorithms for solving urban search and rescue problems? a comparative study with centralized algorithms," *IEEE Transactions on Automation Science and Engineering*, vol. 16, no. 1, pp. 478–485, 2018.

[5] S. Na, H. Niu, B. Lennox, and F. Arvin, "Bio-inspired collision avoidance in swarm systems via deep reinforcement learning," *IEEE Transactions on Vehicular Technology*, 2022.

[6] M. Stefanec, D. N. Hofstadler, T. Krajník, A. E. Turgut, H. Alemdar, B. Lennox, E. Şahin, F. Arvin, and T. Schmickl, "A minimally invasive approach towards "ecosystem hacking" with honeybees," *Frontiers in Robotics and AI*, vol. 9, 2022.

[7] H. Gao, X. Zhang, J. Wen, J. Yuan, and Y. Fang, "Autonomous indoor exploration via polygon map construction and graph-based slam using directional endpoint features," *IEEE Transactions on Automation Science and Engineering*, vol. 16, no. 4, pp. 1531–1542, 2018.

[8] S. Xie, J. Hu, P. Bhowmick, Z. Ding, and F. Arvin, "Distributed motion planning for safe autonomous vehicle overtaking via artificial potential field," *IEEE Transactions on Intelligent Transportation Systems*, vol. 23, no. 11, pp. 21 531–21 547, 2022.

[9] Y. Bian, C. Du, M. Hu, S. E. Li, H. Liu, and C. Li, "Fuel economy optimization for platooning vehicle swarms via distributed economic model predictive control," *IEEE Transactions on Automation Science and Engineering*, 2021.

[10] S. Xie, J. Hu, Z. Ding, and F. Arvin, "Cooperative adaptive cruise control for connected autonomous vehicles using spring damping energy model," *IEEE Transactions on Vehicular Technology*, 2022.

[11] J. Hu, H. Niu, J. Carrasco, B. Lennox, and F. Arvin, "Fault-tolerant cooperative navigation of networked uav swarms for forest fire monitoring," *Aerospace Science and Technology*, p. 107494, 2022.

[12] Y. H. Choi and D. Kim, "Distance-based formation control with goal assignment for global asymptotic stability of multi-robot systems," *IEEE Robotics and Automation Letters*, vol. 6, no. 2, pp. 2020–2027, 2021.

[13] C. J. Stamouli, C. P. Bechlioulis, and K. J. Kyriakopoulos, "Multi-agent formation control based on distributed estimation with prescribed performance," *IEEE Robotics and Automation Letters*, vol. 5, no. 2, pp. 2929–2934, 2020.

[14] Y. Lu, R. Su, C. Zhang, and L. Qiao, "Event-triggered adaptive formation keeping and interception scheme for autonomous surface vehicles under malicious attacks," *IEEE Transactions on Industrial Informatics*, vol. 18, no. 6, pp. 3947–3957, 2021.

[15] J. Hu, B. Lennox, and F. Arvin, "Robust formation control for networked robotic systems using negative imaginary dynamics," *Automatica*, vol. 140, p. 110235, 2022.

[16] Y. Xie, L. Han, X. Dong, Q. Li, and Z. Ren, "Bio-inspired adaptive formation tracking control for swarm systems with application to uav swarm systems," *Neurocomputing*, vol. 453, pp. 272–285, 2021.

[17] M. A. Kamel, X. Yu, and Y. Zhang, "Real-time fault-tolerant formation control of multiple wmrs based on hybrid ga-pso algorithm," *IEEE Transactions on Automation Science and Engineering*, 2020.

[18] G. Guo, P. Li, and L.-Y. Hao, "Adaptive fault-tolerant control of platoons with guaranteed traffic flow stability," *IEEE Transactions on Vehicular Technology*, vol. 69, no. 7, pp. 6916–6927, 2020.

[19] S. Zhao and D. Zelazo, "Bearing rigidity and almost global bearing-only formation stabilization," *IEEE Transactions on Automatic Control*, vol. 61, no. 5, pp. 1255–1268, 2015.

[20] ——, "Localizability and distributed protocols for bearing-based network localization in arbitrary dimensions," *Automatica*, vol. 69, pp. 334–341, 2016.

[21] K. Wu, J. Hu, B. Lennox, and F. Arvin, "Mixed controller design for multi-vehicle formation based on edge and bearing measurements," in *2022 European Control Conference (ECC)*. IEEE, 2022, pp. 1666–1671.

[22] S. Zhao, Z. Li, and Z. Ding, "Bearing-only formation tracking control of multiagent systems," *IEEE Transactions on Automatic Control*, vol. 64, no. 11, pp. 4541–4554, 2019.

[23] Z. Li, H. Tnunay, S. Zhao, W. Meng, S. Q. Xie, and Z. Ding, "Bearing-only formation control with prespecified convergence time," *IEEE Transactions on Cybernetics*, vol. 52, no. 1, pp. 620–629, 2022.

[24] R. Tron, J. Thomas, G. Loianno, K. Daniilidis, and V. Kumar, "A distributed optimization framework for localization and formation control: Applications to vision-based measurements," *IEEE Control Systems Magazine*, vol. 36, no. 4, pp. 22–44, 2016.

[25] M. Basiri, A. N. Bishop, and P. Jensfelt, "Distributed control of triangular formations with angle-only constraints," *Systems & Control Letters*, vol. 59, no. 2, pp. 147–154, 2010.

[26] S. Zhao, F. Lin, K. Peng, B. M. Chen, and T. H. Lee, "Finite-time stabilisation of cyclic formations using bearing-only measurements," *International Journal of Control*, vol. 87, no. 4, pp. 715–727, 2014.
[27] R. Tron, J. Thomas, G. Loianno, K. Daniilidis, and V. Kumar, "Bearing-only formation control with auxiliary distance measurements, leaders, and collision avoidance," in *2016 IEEE 55th Conference on Decision and Control (CDC)*. IEEE, 2016, pp. 1806–1813.
[28] Y.-B. Bae, H.-S. Ahn, and Y.-H. Lim, "Leader-follower bearing-based formation system with exogenous disturbance," in *IEEE International Symposium on Applied Computational Intelligence and Informatics*. IEEE, 2019, pp. 39–44.
[29] Y.-B. Bae, S.-H. Kwon, Y.-H. Lim, and H.-S. Ahn, "Distributed bearing-based formation control and network localization with exogenous disturbances," *International Journal of Robust and Nonlinear Control*, vol. 32, no. 11, pp. 6556–6573, 2022.
[30] T. Xiong and Z. Gu, "Observer-based adaptive fixed-time formation control for multi-agent systems with unknown uncertainties," *Neurocomputing*, vol. 423, pp. 506–517, 2021.
[31] K. Wu, J. Hu, B. Lennox, and F. Arvin, "Finite-time bearing-only formation tracking of heterogeneous mobile robots with collision avoidance," *IEEE Transactions on Circuits and Systems II: Express Briefs*, vol. 68, no. 10, pp. 3316–3320, 2021.
[32] C. Wang, H. Tnunay, Z. Zuo, B. Lennox, and Z. Ding, "Fixed-time formation control of multirobot systems: Design and experiments," *IEEE Transactions on Industrial Electronics*, vol. 66, no. 8, pp. 6292–6301, 2018.
[33] B. Tian, H. Lu, Z. Zuo, and W. Yang, "Fixed-time leader–follower output feedback consensus for second-order multiagent systems," *IEEE Transactions on Cybernetics*, vol. 49, no. 4, pp. 1545–1550, 2018.
[34] M. H. Trinh, D. Mukherjee, D. Zelazo, and H.-S. Ahn, "Finite-time bearing-only formation control," in *2017 IEEE 56th Annual Conference on Decision and Control (CDC)*. IEEE, 2017, pp. 1578–1583.
[35] Q. Van Tran, M. H. Trinh, D. Zelazo, D. Mukherjee, and H.-S. Ahn, "Finite-time bearing-only formation control via distributed global orientation estimation," *IEEE Transactions on Control of Network Systems*, vol. 6, no. 2, pp. 702–712, 2018.
[36] K. Wu, J. Hu, B. Lennox, and F. Arvin, "Sdp-based robust formation-containment coordination of swarm robotic systems with input saturation," *Journal of Intelligent & Robotic Systems*, vol. 102, no. 1, pp. 1–16, 2021.
[37] C. Godsil and G. F. Royle, *Algebraic graph theory*. Springer Science & Business Media, 2013, vol. 207.
[38] H. Khalil, *Nonlinear Systems*. Prentice Hall, 2002.
[39] K. Shojaei, A. M. Shahri, and B. Tabibian, "Design and implementation of an inverse dynamics controller for uncertain nonholonomic robotic systems," *Journal of Intelligent & Robotic Systems*, vol. 71, no. 1, pp. 65–83, 2013.
[40] K. Shojaei and M. Abdolmaleki, "Output feedback control of a tractor with n-trailer with a guaranteed performance," *Mechanical Systems and Signal Processing*, vol. 142, p. 106746, 2020.
[41] M. Zhai, Q. Sun, B. Wang, Z. Liu, and H. Zhang, "Cooperative fault-estimation-based event-triggered fault-tolerant voltage restoration in islanded ac microgrids," *IEEE Transactions on Automation Science and Engineering*, 2022.
[42] X. Li, Y. Zhu, X. Zhao, and J. Lu, "Bearing-based prescribed time formation tracking for second-order multi-agent systems," *IEEE Transactions on Circuits and Systems II: Express Briefs*, 2022.
[43] F. Arvin, J. Espinosa, B. Bird, A. West, S. Watson, and B. Lennox, "Mona: an affordable open-source mobile robot for education and research," *Journal of Intelligent & Robotic Systems*, vol. 94, no. 3, pp. 761–775, 2019.
[44] T. Krajník, M. Nitsche, J. Faigl, T. Duckett, M. Mejail, and L. Přeučil, "External localization system for mobile robotics," in *2013 16th International Conference on Advanced Robotics (ICAR)*. IEEE, 2013, pp. 1–6.

Kefan Wu received B.Sc degree in Applied Mathematics from Lanzhou University in 2016 and M.Sc degree in Applied Mathematics from Wuhan University in 2019. He is currently working toward the Ph.D degree in Electrical and Electronic Engineering at the University of Manchester. His research interests include swarm robotics and control theory.

Junyan Hu received B.Eng degree in Automation from Hefei University of Technology in 2015 and Ph.D degree in Electrical and Electronic Engineering from the University of Manchester in 2020.

Dr. Hu is currently an Assistant Professor with the Department of Computer Science, University College London (UCL). Prior to joining UCL, he worked as a Research Associate in Robotics at the University of Manchester. His research interests include swarm intelligence, multi-agent systems, cooperative path planning, distributed learning and control, with applications to autonomous driving and robotics. He serves as an Associate Editor for IEEE Robotics and Automation Letters and IEEE International Conference on Robotics and Automation. He is a member of IEEE-CSS Technical Committee on Networks and Communication Systems, IEEE-RAS Technical Committee on Multi-Robot Systems, and IFAC Technical Committee on Large Scale Complex Systems.

Zhengtao Ding received the B.Eng. degree from Tsinghua University, Beijing, China, in 1984, and the M.Sc. degree in systems and control, and the Ph.D. degree in control systems from the University of Manchester Institute of Science and Technology, Manchester, U.K. in 1986 and 1989, respectively. After working as a Lecturer with Ngee Ann Polytechnic, Singapore, for ten years, he joined the University of Manchester in 2003, where he is currently Professor of Control Systems with the Dept of Electrical and Electronic Engineering. He is the author of the book: Nonlinear and Adaptive Control Systems (IET, 2013) and has published over 300 research articles. His research interests include nonlinear and adaptive control theory and their applications, more recently network-based control, distributed optimization and distributed machine learning, with applications to power systems and robotics. Prof. Ding has served as an Associate Editor for the IEEE Transactions on Automatic Control, IEEE Control Systems Letters, and several other journals. He is a member of IEEE Technical Committee on Nonlinear Systems and Control, IEEE Technical Committee on Intelligent Control, and IFAC Technical Committee on Adaptive and Learning Systems.

Farshad Arvin received the BSc degree in Computer Engineering, the MSc degree in Computer Systems engineering, and the PhD degree in Computer Science, in 2004, 2010, and 2015, respectively. Farshad is an Associate Professor in Robotics in the Department of Computer Science at Durham University in UK. Prior to that, he was a Senior Lecturer in Robotics at The University of Manchester, UK. He visited several leading institutes including Artificial Life Laboratory with the University of Graz, Institute of Microelectronics, Tsinghua University, Beijing, and Italian Institute of Technology (iit) in Genoa as a Senior Visiting Research Scholar. His research interests include swarm robotics and autonomous multi-agent systems. He is the Founding Director of the Swarm & Computation Intelligence Laboratory formed in 2018, `www.SwaCIL.com`.